

Evidence for Dimer Participation and Evidence Against Channel Mechanism in A23187-Mediated Monovalent Metal Ion Transport Across Phospholipid Vesicular Membrane

B. S. Prabhananda and Mamata H. Kombrabail

Department of Chemical Sciences, Tata Institute of Fundamental Research, Mumbai 400 005, India

ABSTRACT The decay of the pH difference (ΔpH) across soybean phospholipid vesicular membrane by ionophore A23187 (CAL)-mediated H^+/M^+ exchange ($\text{M}^+ = \text{Li}^+, \text{Na}^+, \text{K}^+, \text{and Cs}^+$) has been studied in the pH range 6–7.6. The ΔpH in these experiments were created by temperature jump. The observed dependence of ΔpH relaxation rate $1/\tau$ on the concentration of CAL, pH, and the choice of M^+ in vesicle solutions lead to the following conclusions. 1) The concentrations of dimers and other oligomers of A23187 in the membrane are small compared to the total concentration of A23187 in the membrane, similar to that in chloroform solutions reported in the literature. 2) In the H^+ transport cycle leading to ΔpH decay, the A23187-mediated H^+ translocation across the membrane is a fast step, and the rate-limiting step is the A23187-mediated M^+ translocation. 3) Even though the monomeric Cal-H is the dominant species translocating H^+ , Cal-M is not the dominant species translocating M^+ (even at concentrations higher than $[\text{Cal-H}]$), presumably because its dissociation rate is much higher than its translocation rate. 4) The pH dependence of $1/\tau$ shows that the dimeric species Cal_2LiLi , Cal_2NaNa , Cal_2KH , and Cal_2CsH are the dominant species translocating M^+ . The rate constant associated with their translocation has been estimated to be $\sim 5 \times 10^3 \text{ s}^{-1}$. With this magnitude for the rate constants, the dimer dissociation constants of these species in the membrane have been estimated to be $\sim 4, 1, 0.05, \text{ and } 0.04 \text{ M}$, respectively. 5) Contrary to the claims made in the literature, the data obtained in the ΔpH decay studies do not favor the channel mechanism for the ion transport in this system. 6) However, they support the hypothesis that the dissociation of the divalent metal ion-A23187 complex is the rate limiting step of A23187-mediated divalent metal ion transport.

INTRODUCTION

The antibiotic A23187 (calcimycin, or CAL) has been extensively used in biochemical research because of its ability to facilitate transmembrane Ca^{2+} ion transport. Initially, this ionophore was thought to be specific for divalent metal ions (Reed and Lardy, 1972). However, there is now ample experimental evidence for CAL-mediated monovalent metal ion (M^+) transport, such as that of K^+ ion also (Pfeiffer and Lardy, 1976; Ben-Hayyim and Krause, 1980; Nakashima and Garlid, 1982; Garlid et al., 1986; Krishnamoorthy and Ahmed, 1992; Ortiz-Carranza et al., 1997). Presumably, such a transport is responsible for CAL-mediated K^+/H^+ exchange and $2\text{K}^+/\text{Ca}^{2+}$ exchange across membranes. In the literature, there have been suggestions that CAL-mediated K^+/H^+ exchange is similar to that by nigericin and that the dimeric species Cal_2MH is dominantly responsible for the transmembrane M^+ transport (Pfeiffer and Lardy, 1976). The species Cal_2M^- have also been suggested to be

transporting M^+ across the membrane (Krishnamoorthy and Ahmed, 1992). In the present work we have tested such hypotheses by kinetic measurements using $\text{M}^+ = \text{Li}^+, \text{Na}^+, \text{K}^+, \text{and Cs}^+$. A recent controversy about the existence of CAL oligomers and the channel mechanism in CAL facilitated transmembrane H^+/M^+ transport (Balasubramanian et al., 1992; Jyoti et al., 1994; Prabhananda and Kombrabail, 1994; Thomas et al., 1997) has also been examined. Our experimental strategy is based on the following.

In liposomes transmembrane H^+ transport can be driven by a pH difference across the membrane (ΔpH). However, a net H^+ transport in one direction generates electric potential across the membrane that opposes further H^+ transport. Therefore, for continued H^+ conduction leading to ΔpH decay in liposomes, it is necessary to abolish this electric potential by a compensating charge flux such as that from alkali metal ion transport in the opposite direction (Henderson et al., 1969). From a study of the dependence of ΔpH decay rate on various concentrations we can identify the rate-limiting species. For example, when the rate-limiting step involves CAL-species the ΔpH decay rate will show a dependence on the concentration of CAL. When the H^+ transport step is sufficiently fast and the ΔpH decay rate is limited by the M^+ transport step, the CAL-species transporting M^+ across the membrane can be identified by the above procedure. In our experiments, soybean phospholipid (SBPL) vesicles were used as model membranes for reasons mentioned elsewhere, and temperature jump (T-jump) was used to create ΔpH across the vesicular membrane (Krishnamoorthy, 1986; Prabhananda and Ugrankar, 1991).

Received for publication 2 December 1997 and in final form 26 May 1998.

Address reprint requests to Dr. B. S. Prabhananda, Department of Chemical Sciences, Tata Institute of Fundamental Research, Mumbai 400 005, India. Tel.: 91-22-2152971; Fax: 91-22-2152110; E-mail: bsp@tifrvax.tifr.res.in.

Abbreviations used: Cal-H, protonated A23187 monomer; Cal-M, monovalent metal ion-bound A23187 monomer; $\text{Cal}_2\text{-DM}$, divalent metal ion-bound A23187 dimer; Cal_2XY , A23187 dimer to which monovalent cations X^+ and Y^+ are bound.

© 1998 by the Biophysical Society

0006-3495/98/10/1749/10 \$2.00

MATERIALS AND METHODS

The SBPL vesicle solutions with 2 mM pyranine inside and other concentration conditions as given in the figure legends were prepared from asolectin (Sigma, St. Louis, MO), following the procedure described elsewhere (Krishnamoorthy, 1986; Prabhananda and Ugrankar, 1991). In our experiments MCl ($M^+ = \text{Li}^+, \text{Na}^+, \text{K}^+, \text{and Cs}^+$) were used to regulate concentrations of M^+ in the SBPL vesicle solutions. Concentrated HCl and MOH were used to adjust the pH of the *N*-(acetamido)-2-aminoethanesulfonic acid (ACES) and tris(hydroxymethyl)aminomethane (TRIS) + ACES buffers. Stock solutions of 5 mM CAL (Sigma) in ethanol were added in microliter amounts to vesicle solutions with vortex stirring. T-jump was used to create ΔpH (~ 0.02) and the ΔpH decay was observed at $23 \pm 1.5^\circ\text{C}$ by monitoring the fluorescence from the pH indicator pyranine entrapped inside vesicles (Prabhananda and Ugrankar, 1991). The observed ΔpH decay traces were single exponentials. The ΔpH relaxation times τ were measured by comparing the observed trace with those obtained from a calibrated exponential generator (Prabhananda and Ugrankar, 1991).

RESULTS

Dependence of ΔpH relaxation rate on CAL concentration

The CAL added to SBPL vesicle solutions is predominantly partitioned to the vesicular membrane. Therefore, in the absence of oligomer formation its concentration in the inner layer of the membrane, $[\text{Cal}]_{\text{il}}$, can be related to lipid concentration ($[\text{lip}]$) and the concentration $[\text{Cal}]_0$ estimated with respect to vesicle solution volume (Prabhananda and Ugrankar, 1991).

$$[\text{Cal}]_{\text{il}} = 0.95[\text{Cal}]_0/[\text{lip}] \text{ M.} \quad (1)$$

When a specific step of the H^+/M^+ transport cycle dominantly limits the ΔpH decay rate in vesicle solutions, the ΔpH relaxation rate $1/\tau$ is linearly related to the concentration of the rate-limiting species (Prabhananda and Ugrankar, 1991; Prabhananda and Kombrabail, 1996):

$$1/\tau \approx (\ln 10)k[\text{rate limiting species}]_{\text{il}}/b_i \quad (2)$$

where k is the rate constant and b_i is the internal buffer capacity of vesicles.

$$b_i = (\ln 10)\{\sum C_j K_{\text{Hj}}[\text{H}^+]/(K_{\text{Hj}} + [\text{H}^+])^2\} \quad (3)$$

where C_1 and K_{H1} are the concentration and proton dissociation constant of the buffers entrapped inside vesicles. $C_2 = 30 \text{ mM}$, $K_{\text{H2}} = 10^{-6.9} \text{ M}$, $C_3 = 45 \text{ mM}$, and $K_{\text{H3}} = 10^{-7.8} \text{ M}$ are associated with the endogenous groups in SBPL vesicles (Prabhananda and Kombrabail, 1992).

In view of Eq. 2 we can say that the nature of the CAL-species participating in the rate-limiting step of ΔpH decay for different choices of M^+ can be inferred from the dependence of $1/\tau$ on $[\text{Cal}]_0$ and pH. From the observed near-linear increase of $1/\tau$ with $[\text{Cal}]_0^2$ (Fig. 1) we can infer that the concentration of the rate-limiting species is nearly proportional to $[\text{Cal}]_0^2$ or $[\text{Cal}]_{\text{il}}^2$. Such a situation can be envisaged only if 1) the rate-limiting species is made up of two CAL molecules, 2) $[\text{rate-limiting species}]_{\text{il}} \ll [\text{Cal}]_{\text{il}}$, and 3) the dimeric rate-limiting species is in a dynamic

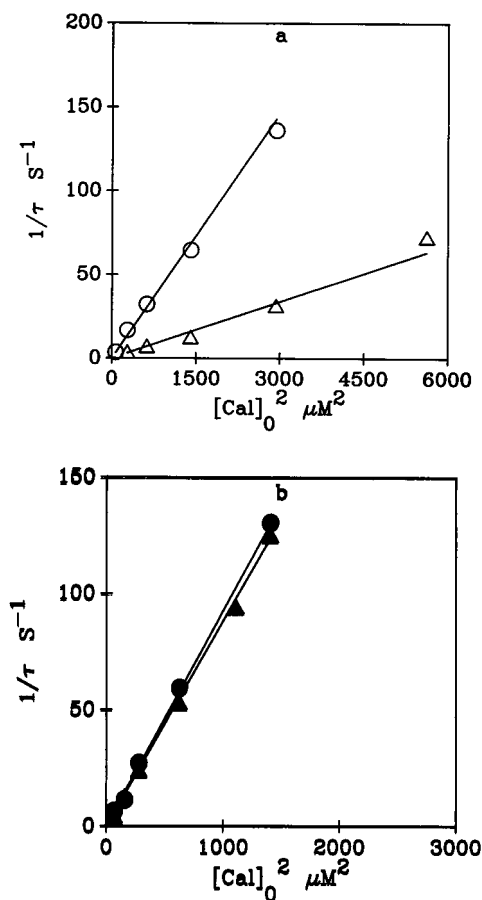
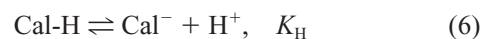


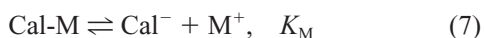
FIGURE 1 Dependence of ΔpH relaxation rate $1/\tau$ on A23187 concentration, $[\text{Cal}]_0$, in SBPL vesicle solutions containing 100 mM MCl at pH 7. $M^+ =$ (a) Li^+ , Δ ; Na^+ , \circ ; (b) K^+ , \bullet ; Cs^+ , \blacktriangle . Inside vesicles 0.25 mM ACES buffer. Outside vesicles 7 mM ACES for Li^+ , Na^+ , and K^+ ; 7 mM ACES + 10 mM TRIS for Cs^+ . Lipid concentrations were (a) 3.5 mM for Li^+ and Na^+ , and (b) 3.3 mM for K^+ and 3.2 mM for Cs^+ .

equilibrium with the monomeric CAL-species. The dependence of the slopes of the plots in Fig. 1 on the specific choice of M^+ suggests the involvement of the metal ion in the constitution of the rate-limiting species. The dynamic equilibria of the two possible dimeric species in the membrane showing such features are given below.



The magnitudes of the dissociation constants K_{MH} and K_{MM} of the above equilibria are such that the concentrations of the dimeric species $[\text{Cal}_2\text{MH}]$ and $[\text{Cal}_2\text{MM}]$ are very much less than $[\text{Cal}]_{\text{il}}$, as mentioned above. The apparent dissociation constants K_{H} and K_{M} of the following equilibria refer to those determined with concentrations of the CAL-species in the membrane and $[\text{H}^+]$ and $[\text{M}^+]$ in the aqueous medium. $[\text{H}^+]$ and M^+ bind to CAL competitively; see Eq. 5 of Pfeiffer and Lardy (1976)].





Therefore, the concentrations of the above-mentioned candidates for the rate-limiting species of ΔpH decay can be calculated using the following expressions.

$$[\text{Cal}_2\text{MH}]_{\text{il}} = (K_H/K_M)(1/K_{\text{MH}})[\text{Cal}]_{\text{il}}^2[\text{H}^+][\text{M}^+]/A^2 \quad (8)$$

$$[\text{Cal}_2\text{MM}]_{\text{il}} = (K_H/K_M)^2(1/K_{\text{MM}})[\text{Cal}]_{\text{il}}^2[\text{M}^+]^2/A^2 \quad (9)$$

$$A \approx \{K_H + [\text{H}^+] + [\text{M}^+](K_H/K_M)\} \quad (10)$$

Dependence of τ on pH

The dependence of $1/\tau$ on pH comes from 1) b_i (Eq. 3), and 2) concentration of the rate-limiting species (Eqs. 8 or 9) occurring in the expression for $1/\tau$ (Eq. 2). Since the variation of the concentrations with $[\text{H}^+]$ predicted by Eqs. 8 and 9 are distinctly different, we should be able to identify the rate-limiting species as either Cal_2MH or Cal_2MM from the pH dependence of $1/\tau$. The estimate of K_H in typical phospholipid vesicles is $\sim 10^{-7.8}$ M (Kauffman et al., 1982). Therefore, for a given vesicle preparation in the pH range of our study (especially in the lower pH region) the “shape” of the $1/\tau$ against pH plots is mainly decided by the magnitude of K_H/K_M and the nature of the rate-limiting species (Eqs. 2, 8, and 9). The parameters k/K_{MH} or k/K_{MM} can be suitably chosen to match the magnitudes of the observed τ with the calculated τ .

Fig. 2 shows the variation of CAL-facilitated $1/\tau$ with pH. The “shape” of the plot for the data obtained with Li^+ as the alkali metal ion in vesicle solutions is close to that of $0.5/b_i$ against pH (Fig. 2 a). Such an observation implies only a small variation of the concentration of rate-limiting species with pH (in our pH range) and helps us identify Cal_2LiLi as the rate-limiting species in this system (see Eq. 2). The experimental “shape” of the data obtained with Li^+ as the metal ion (Fig. 2 a) could be reproduced using Eqs. 2 and 9 for $K_H/K_{\text{Li}} = 10^{-4.4}$, a value close to that expected from the dissociation constants determined by Kauffman et al. (1982) and Taylor et al. (1985). The $1/\tau$ data obtained with Na^+ as the metal ion (shown in Fig. 2 a) does not show significant variation with pH. Such a “shape” could be explained by identifying the Cal_2NaNa as the rate-limiting species with $K_H/K_{\text{Na}} = 10^{-5}$. The ratio of the apparent dissociation constants $K_{\text{Na}}/K_{\text{Li}} (=10^{0.6})$ in SBPL vesicles determined from these estimates is close to that in aqueous methanol reported in the literature (Taylor et al., 1985). However, this estimate is an order of magnitude smaller than in L- α -Dimyristoylphosphatidylcholine (DMPC) vesicles, presumably due to differences in the lipid composition (Taylor et al., 1985). (Calculations using $K_H/K_{\text{Na}} < 10^{-5.5}$ predicted a substantial increase in $1/\tau$ with pH quite different from the observed shape. Such a trend can also be seen in the broken line of Fig. 2 b obtained from such a calculation.) However, the data obtained with K^+ and Cs^+ could be reproduced only in the lower pH regions if Cal_2KK or Cal_2CsCs is assumed to be the rate-limiting species (see the broken line

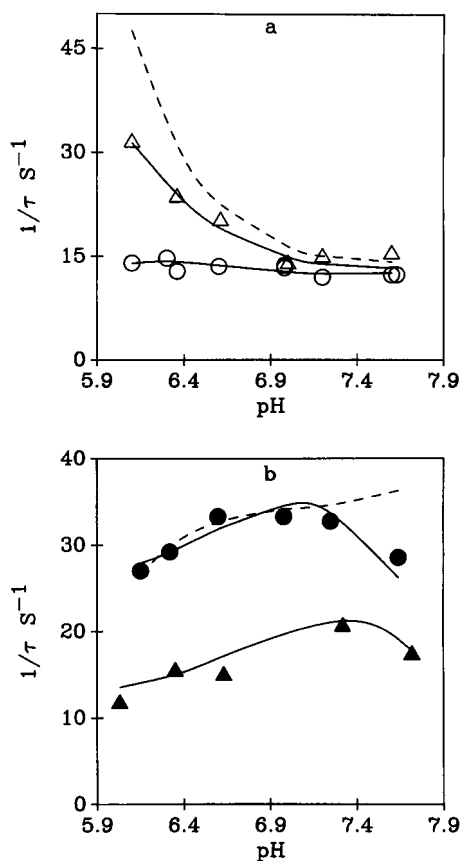


FIGURE 2 pH dependence of $1/\tau$ observed in SBPL vesicle solutions containing 100 mM MCl for different choices of monovalent metal ions. $\text{M}^+ =$ (a) Li^+ , Δ ; Na^+ , \circ ; (b) K^+ , \bullet ; Cs^+ , \blacktriangle . The concentrations $[\text{Cal}]_0$ were (a) 33 μM and 17 μM , and (b) 17 μM and 12.5 μM , respectively. Buffers and lipid concentrations were the same as those used in obtaining the data of Fig. 1. The broken line in (a) corresponds to $1/\tau = 0.5/b_i$ plotted against pH; the broken line in (b) corresponds to calculated pH dependence, fitting the data at lower pH conditions using $K_H/K_M = 10^{-5.2}$ and assuming Cal_2KK to be the rate-limiting species. Solid lines were calculated using Eq. A7 and the parameters given in Table 1 with rate-limiting species as identified in the text.

simulated using $K_H/K_M = 10^{-5.2}$ and other constants appropriately chosen to fit the lower pH region of the $\text{M}^+ = \text{K}^+$ data in Fig. 2 b). The shapes of the plots in Fig. 2 b could be reproduced only by identifying Cal_2KH and Cal_2CsH as the rate-limiting species and using K_H/K_M comparable to that given in Table 1.

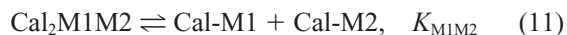
TABLE 1 Parameters determined from the observed dependence of $1/\tau$ on $[\text{Cal}]_0$ and on pH using Eqs. 8, 9, and A7 with $f_x = 1$ for Li^+ and Na^+ and $f_x = 0$ for K^+ and Cs^+

Metal Ion	K_H/K_M	$k_2/K_{\text{MM}} (\text{M}^{-1} \text{s}^{-1})$	$k_1/K_{\text{MH}} (\text{M}^{-1} \text{s}^{-1})$
Li^+	$10^{-4.4}$	1.3×10^3	
Na^+	10^{-5}	5.0×10^3	
K^+	$10^{-6.3}$		10×10^4
Cs^+	$10^{-6.5}$		12×10^4

$1/\tau$ could also be fitted using $f_x = 0.92$, $K_H/K_M = 10^{-5.4}$, $k_2/K_{\text{MM}} = 5.5 \times 10^3 \text{ M}^{-1} \text{s}^{-1}$ for $\text{M}^+ = \text{Na}^+$ and using $f_x = 0.18$, $k_1/K_{\text{MH}} = 12 \times 10^4 \text{ M}^{-1} \text{s}^{-1}$ for $\text{M}^+ = \text{K}^+$.

Confirmation of the rate-limiting species from experiments in a mixture of metal ions

If the dimeric species Cal_2MM can exist, as inferred above, species of the type $\text{Cal}_2\text{M1M2}$ can also be expected to exist with dissociation constant K_{M1M2} in the membrane when two types of metal ions M1^+ and M2^+ are in vesicle solutions.



The concentrations of Cal-M1 and Cal-H in this case are given by the following expressions.

$$[\text{Cal-M1}]_{\text{il}} = (K_{\text{H}}/K_{\text{M1}})[\text{Cal}]_{\text{il}}[\text{M1}^+]/A^*$$

$$[\text{Cal-H}]_{\text{il}} = [\text{Cal}]_{\text{il}}[\text{H}^+]/A^* \quad (12)$$

$$A^* \approx \{K_{\text{H}} + [\text{H}^+] + [\text{M1}^+](K_{\text{H}}/K_{\text{M1}}) + [\text{M2}^+](K_{\text{H}}/K_{\text{M2}})\} \quad (13)$$

A similar expression can be written for $[\text{Cal-M2}]_{\text{il}}$. Thus, if our identification of the rate-limiting species is correct, in vesicle solutions containing $\text{M1}^+ = \text{Li}^+$ and $\text{M2}^+ = \text{Na}^+$ the CAL-facilitated $1/\tau$ should include contributions from $[\text{Cal}_2\text{M1M2}]_{\text{il}}$ in addition to that from $[\text{Cal}_2\text{M1M1}]_{\text{il}}$ ($=1/\tau_{\text{M1}}$) and $[\text{Cal}_2\text{M2M2}]_{\text{il}}$ ($=1/\tau_{\text{M2}}$). $1/\tau_{\text{M1}}$ and $1/\tau_{\text{M2}}$ can be calculated with A^* instead of A (Eq. 13) in Eqs. 2 and 9 using the parameters given in Table 1. Since $[\text{Cal}_2\text{M1M2}]_{\text{il}}$ is proportional to the product $[\text{Cal-M1}]_{\text{il}} \times [\text{Cal-M2}]_{\text{il}}$ it should be possible to express the above-mentioned additional contribution to $1/\tau$ using an equation similar to Eq. 2,

$$\{1/\tau - 1/\tau_{\text{Li}} - 1/\tau_{\text{Na}}\} = F_{\text{ext}} \times [\text{Cal-Li}]_{\text{il}} \times [\text{Cal-Na}]_{\text{il}}/b_i \quad (14)$$

with a constant value for F_{ext} (proportional to the rate constant). The significant and near-constant F_{ext} for $\text{M1}^+ = \text{Li}^+$ and $\text{M2}^+ = \text{Na}^+$ seen in Table 2 confirm this prediction.

Cal_2MH has been identified to be the rate-limiting species for $\text{M}^+ = \text{K}^+$ or Cs^+ . Therefore, in vesicle solutions containing a mixture of K^+ and Cs^+ we can expect dominant contributions to CAL-facilitated $1/\tau$ to come from $[\text{Cal}_2\text{KH}]_{\text{il}}$ ($=1/\tau_{\text{K}}$) and $[\text{Cal}_2\text{CsH}]_{\text{il}}$ ($=1/\tau_{\text{Cs}}$) and negligible

contributions to come from $[\text{Cal}_2\text{M1M2}]$ ($\text{M1}^+, \text{M2}^+ = \text{K}^+$ and Cs^+). (In the calculations of these contributions using Eqs. 2 and 8 one must use A^* instead of A .) The data given in Table 2 for the K^+ and Cs^+ mixed ion system also confirm this prediction.

Identification of the rate-limiting step

The relaxation rates $1/\tau_{\text{b}}$ associated with the equilibration of the bimolecular reactions $X + Y \rightleftharpoons W + Z$ or $X + Y \rightleftharpoons X - Y$, with rate constants k_{f} and k_{r} in the forward and reverse directions, depend on the concentrations of the reactants (Eigen and DeMayer, 1963).

$$1/\tau_{\text{b}} = k_{\text{f}}\{[X] + [Y]\} + k_{\text{r}}\{[W] + [Z]\}$$

$$\text{or } 1/\tau_{\text{b}} = k_{\text{f}}\{[X] + [Y]\} + k_{\text{r}} \quad (15)$$

The transfers of H^+/M^+ between the aqueous medium and the CAL-species in the membrane can be considered to be bimolecular reactions at the interface. The equilibration rate for this step should not show a significant dependence on $[\text{Cal}]_0$, since at the interface it is mainly determined by the concentrations of the buffer species and M^+ , which are large compared to $[\text{Cal}]_0$. Thus, the observed τ is not associated with this fast step.

If the translocation of the M^+ carriers Cal_2MM or Cal_2MH is the rate-limiting step it must be possible to increase the translocation rates (and $1/\tau$) by disturbing the membrane order such as by adding valinomycin at sufficiently high concentrations (Prabhananda and Kombrabail, 1995). The ΔpH relaxation traces shown in Fig. 3 a with $\text{M}^+ = \text{Li}^+$ and in Fig. 3 b with $\text{M}^+ = \text{K}^+$ confirm this prediction. The following two observations show that the increase of $1/\tau$ was not due to increased M^+ transport by valinomycin. 1) Similar magnitudes of changes were observed with both $\text{M}^+ = \text{Li}^+$ and K^+ even though the selectivity of valinomycin to K^+ transport is relatively high. 2) There was no increase in $1/\tau$ on increasing M^+ transport by forming gramicidin channels in the membrane.

TABLE 2 τ data and concentration of monomeric CAL-species in SBPL vesicle solutions containing a mixture of M1Cl and M2Cl such that $[\text{M1Cl}] + [\text{M2Cl}] = 0.1 \text{ M}$

Ions	$[\text{M1}]_0$ (M)	$[\text{M2}]_0$ (M)	$[\text{Cal-H}]_{\text{il}}$ (mM)	$[\text{Cal-M1}]_{\text{il}}$ (mM)	$[\text{Cal-M2}]_{\text{il}}$ (mM)	τ (ms)	τ_{x}^* (ms)	$F_{\text{ext}}^{\#}$
$\text{M1} = \text{Li}^+$	0.025	0.075	0.36	3.62	2.73	38	115	21
$\text{M2} = \text{Na}^+$	0.050	0.050	0.26	5.17	1.30	57	170	20
	0.075	0.025	0.20	6.03	0.51	77	161	26
$\text{M1} = \text{K}^+$	0.017	0.083	2.23	0.19	0.59	63	66	
$\text{M2} = \text{Cs}^+$	0.050	0.050	2.14	0.54	0.34	59	63	
	0.083	0.017	2.06	0.86	0.11	63	61	

The buffers were 0.25 mM ACES inside vesicles and 7 mM ACES (with $\text{Li}^+ + \text{Na}^+$ ions) or 7 mM ACES + 10 mM TRIS (with $\text{K}^+ + \text{Cs}^+$ ions) outside vesicles at pH = 7. The concentrations of monomeric CAL-species were estimated neglecting the concentrations of dimeric species and using the parameters given in Table 1 in Eqs. 12 and 13. The concentrations $[\text{lip}]$ and $[\text{Cal}]_0$ were 3.5 mM and 25 μM in the $\text{Li}^+ + \text{Na}^+$ mixed ion system and 3.4 mM and 12 μM in the $\text{K}^+ + \text{Cs}^+$ mixed ion system.

* $1/\tau_{\text{x}} = 1/\tau_{\text{M1}} + 1/\tau_{\text{M2}}$.

$^{\#}F_{\text{ext}} = b_i \times \{1/\tau - 1/\tau_{\text{x}}\}/\{[\text{Cal-M1}]_{\text{il}} \times [\text{Cal-M2}]_{\text{il}}\}$. See Eq. 14.

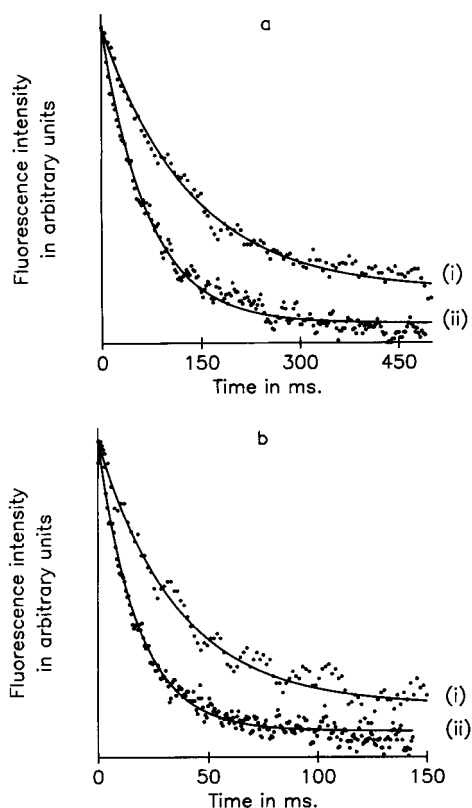


FIGURE 3 (a) A23187-mediated ΔpH relaxation traces observed with 100 mM LiCl in 3.5 mM SBPL vesicle solutions at pH ~ 7 and $[\text{Cal}]_0 = 25 \mu\text{M}$. (i) $[\text{Valinomycin}]_0 = 0$, $\tau = 135$ ms, and (ii) $[\text{valinomycin}]_0 = 84 \mu\text{M}$, $\tau = 70$ ms. (b) ΔpH relaxation traces observed with 100 mM KCl in 3.5 mM SBPL vesicle solutions at pH ~ 6.35 and $[\text{Cal}]_0 = 17 \mu\text{M}$. (i) $[\text{Valinomycin}]_0 = 0$, $\tau = 36$ ms, and (ii) $[\text{valinomycin}]_0 = 84 \mu\text{M}$, $\tau = 18$ ms. Buffer details are similar to those given for Fig. 1.

DISCUSSION

CAL-mediated transmembrane H^+/M^+ transport scheme

The CAL-species inferred above and the conclusions given above suggest the ion transport scheme of Fig. 4 for the

CAL-facilitated ΔpH decay. In this scheme the Cal_2MH could be considered as H^+ carrier if the dominant reaction of this species at the “interface” is the fast H^+/M^+ exchange leading to the formation of Cal_2MM :



with dissociation of Cal_2MM given by Eq. 5. However, Cal_2MH could be considered as M^+ carrier if instead of Eq. 16 the dominant reaction of Cal_2MH at the interface is the fast M^+/H^+ exchange leading to the formation of Cal_2HH , which dissociates into monomers.



The expression for $1/\tau$ has been derived in the Appendix (Eq. A7) using the transport scheme of Fig. 4 and taking note of the aforementioned uncertainty with the help of the factor f_x : f_x is the probability of the reaction given in Eq. 16. Eq. A7 is consistent with the observed behaviors of τ since it reduces to Eq. 2, with [rate-limiting species]_{ii} given by Eq. 8 or 9 depending on the choice of M^+ . With the stronger binding metal ions Li^+ and Na^+ , the dissociation of M^+ from Cal_2MH may be more difficult than that of H^+ making Eq. 16 more probable and $f_x = 1$. Similarly, with weaker binding metal ions K^+ and Cs^+ , Eq. 17 and $f_x = 0$ may be appropriate. When $\text{M}^+ = \text{Li}^+$ or Na^+ we have inferred that the H^+ translocation is not rate-limiting. Thus, in Eq. A7 the term involving k_2 (associated with M^+ translocation) should be negligible compared to the terms involving k_0 and k_1 (associated with H^+ translocation). Therefore, $[\text{H}^+]_i \{k_0 + 2k_1[\text{Cal}]_{ii}/A\} ([\text{M}^+]/K_{\text{MH}})(K_{\text{H}}/K_{\text{M}}) \gg 2(k_2/K_{\text{MM}})[\text{Cal}]_{ii}/A ([\text{M}^+]/K_{\text{H}}/K_{\text{M}})^2$. Also, we can use Eq. 12 with $K_{\text{H}}/K_{\text{M}}$ given in Table 1 to show that the concentration of H^+ translocating species $[\text{Cal-H}]_{ii}$ in the experiments with $\text{M}^+ = \text{K}^+$ or Cs^+ are much greater than that with Li^+ or Na^+ . Thus, if H^+ translocation is not limiting the rate of ΔpH decay for $\text{M}^+ = \text{Li}^+$ or Na^+ it must be a even faster step and $F_4 \approx k_0 \times [\text{H}^+]_{ii}$ in Eq. A7 when $\text{M}^+ = \text{K}^+$ or

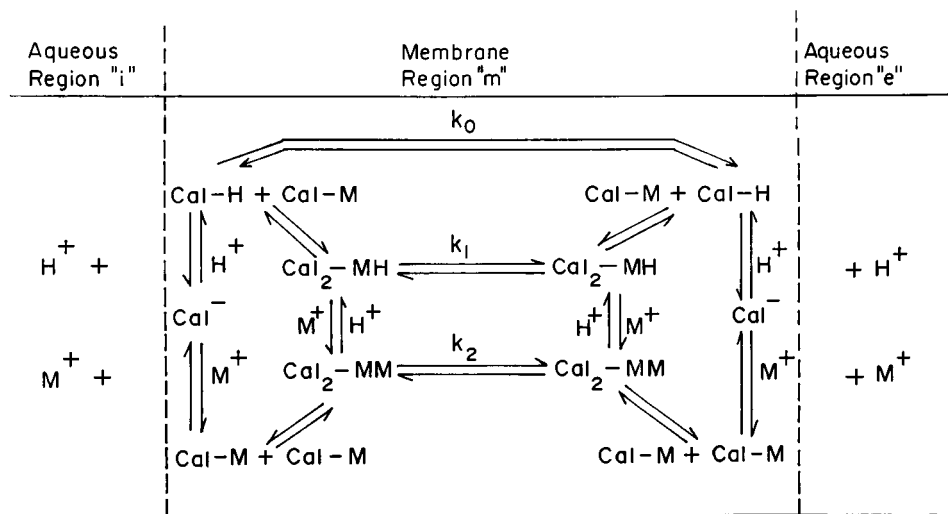


FIGURE 4 Suggested transport scheme for the dominant mode of A23187-mediated ΔpH decay with monovalent metal ion transport participation.

Cs^+ . Estimates of k_2/K_{MM} and k_1/K_{MH} which reproduce the observed magnitudes of $1/\tau$ on using the above conditions in Eq. A7 are given in Table 1.

It is possible to choose f_x slightly different from (but close to) 1 and 0 and yet obtain calculated τ in agreement with the observed τ within the limits of errors for $\text{M}^+ = \text{Na}^+$ and K^+ ions. Typical sets of parameters used for obtaining such τ are given in the footnote of Table 1.

Estimates of translocation rate constants and dimer dissociation constants

Equation A7 and the $1/\tau$ data are not adequate to determine unique estimates of the translocation rate constants of the transport scheme (Fig. 4) and the dimer dissociation constants of the reactions given in Eqs. 4 and 5. However, we can get the limits to their magnitudes using the following criteria. 1) To get the linear behaviors seen in Fig. 1 within the limits of experimental errors, $[\text{Cal}_2\text{MM}]_{\text{il}}$ and $[\text{Cal}_2\text{MH}]_{\text{il}}$ should be $<10\%$ of the $[\text{Cal}]_{\text{il}}$ even at the highest $[\text{Cal}]_{\text{il}}$. Using this restriction in Eq. 9 we get $K_{\text{MM}} > 0.15 \text{ M}$ and $> 0.2 \text{ M}$ along with $k_2 > 5 \times 10^2 \text{ s}^{-1}$ and $> 10^3 \text{ s}^{-1}$ for $\text{M}^+ = \text{Li}^+$ and Na^+ , respectively. Similarly, we can use Eq. 8 to conclude that $K_{\text{MH}} > 0.02 \text{ M}$ and $k_1 > 2 \times 10^3 \text{ s}^{-1}$ for $\text{M}^+ = \text{K}^+$ and Cs^+ . 2) The translocation rate constants of Cal_2MH and Cal_2MM are unlikely to be much different from those of other electroneutral molecules of similar molecular weight and size, such as the metal ion-bound monensin (Prabhananda and Kombrabail, 1992) or nigericin (Prabhananda and Ugrankar, 1991). Using this criterion we get 10^4 s^{-1} as the upper limit for k_1 and k_2 . Choosing $k_1 = k_2 \sim 5 \times 10^3 \text{ s}^{-1}$ between the two limits given above, we get $K_{\text{MM}} \sim 4 \text{ M}$ and 1 M for $\text{M}^+ = \text{Li}^+$ and Na^+ . Also, $K_{\text{MH}} \sim 0.05 \text{ M}$ and 0.04 M for K^+ and Cs^+ . 3) The CAL-mediated H^+ translocation step (as Cal-H translocation) is sufficiently faster than the M^+ translocation step. This condition is satisfied if $k_0 \gg k_2$ (say $k_0 \sim 10^5 \text{ s}^{-1}$). Such an estimate is consistent with the inequality $k_0 \geq 28 \text{ s}^{-1}$ given by Kolber and Haynes (1981). They had observed that when a solution of vesicles loaded with Ca^{2+} is mixed with a solution containing CAL and ethylenediaminetetraacetic acid (EDTA) the ionophore fluorescence increase with time is biexponential. The fast phase of this change could be attributed to the overall process in which CAL is incorporated into the membrane from the aqueous medium and is equilibrated across the two layers of the membrane. In view of our estimate of k_0 given above we can say that the incorporation of CAL from the aqueous medium into the membrane (which could involve a fast binding to the surface followed by a slower step of distortion of the membrane structure at the interface to accommodate the ionophore) is slow compared to the translocation of Cal-H involved in the equilibration across the membrane. 4) The data for $\text{M}^+ = \text{K}^+$ and Cs^+ (Fig. 2) require the dominant M^+ translocation term in the expression for $1/\tau$ to be proportional to $[\text{Cal}_2\text{MH}]_{\text{il}}$ even though Cal_2MM can also

translocate M^+ . Therefore, in these situations we should have $[\text{Cal}_2\text{MH}]_{\text{il}} \gg [\text{Cal}_2\text{MM}]_{\text{il}}$ since $k_1 \approx k_2$. Substituting the smallest $[\text{H}^+]$ of our experiments and setting the detectable limit of the less dominant term as 10% of the dominant term in Eq. A7 (and with $f_x = 0$ and $F_4 \approx k_0 [\text{H}^+]_{\text{i}}$) we get $0.05 K_{\text{MM}} > K_{\text{MH}}$. Thus, K_{KK} and $K_{\text{CsCs}} > 1 \text{ M}$. 5) With intermolecular interactions contributing to the dominant stability of the dimeric species we should not expect large differences in the magnitudes of K_{MM} for different choices of M^+ . The estimates given above are consistent with such an expectation. The differences between K_{MH} and K_{MM} could be the result of structural differences, steric factors, and hydrogen bond bridges favoring the stability of Cal_2MH . 6) In our transport scheme the dominant fast step of H^+ translocation is by Cal-H translocation. The possibility of a dominant H^+ translocation by the dimeric Cal_2HH with translocation rate constant k_0^* ($\approx k_1$ in view of the similarity in the sizes of dimeric species) is not compatible with the requirement on the relative concentrations of monomeric and dimeric species. (See Discussion about modification of Eqs. A7 and A8 in the Appendix). 7) A paradoxical feature of the transport scheme (Fig. 4) is that to explain the $1/\tau$ data we require the translocation rate constant of monomeric Cal-M to be negligible even though the translocation rate constant of the monomeric Cal-H is high. This paradox can be understood if the M^+ dissociation rate constant of Cal-M in the membrane is so high that it dissociates even before its translocation across the membrane, unlike the situations with the dimeric Cal_2MH and Cal_2MM . 8) In Fig. 4, the rate of ΔpH decay involves H^+ translocation by the monomeric Cal-H and the M^+ translocation is by the dimeric species. Therefore, it follows that the rate of equilibration between the monomeric and dimeric species in the membrane must be faster than $1/\tau$. Also, for the efficient translocation of M^+ , the dimer dissociation rate constant should be $\ll k_1, k_2$.

CAL species inferred from experiments

The monomeric species Cal^- , Cal-H, and Cal-M invoked for the above discussion of the kinetic data have been inferred from optical absorption or fluorescent studies (Kauffman et al., 1982; Pfeiffer et al., 1974; Taylor et al., 1985) and using two phase extraction technique (Pfeiffer and Lardy, 1976). The dimeric species Cal_2MH invoked to explain the data of the latter studies could not be inferred from the two phase extraction data obtained with $\text{M}^+ = \text{Li}^+$, Na^+ , K^+ , and Cs^+ by Mimouni et al. (1992) even though they had used a higher concentration of CAL ($\sim 2 \text{ mM}$ in the organic phase). Our conclusions about the "dimeric species" can be reconciled with the two-phase extraction data as explained below: in our experiments the total concentration of CAL in the lipid membrane (estimated using Eq. 1) was 3–10 mM. Even though we invoke the dimeric species to explain the kinetic data, we require their concentrations to be considerably smaller than those of

monomeric species to explain the linear plots of Fig. 1. Presumably, the errors in the two-phase extraction data make it difficult to detect the dimeric species at small concentrations in the presence of monomeric species at large concentrations. However, on using $M = \text{Ag}$ and Hg (for which the selectivity of CAL is quite high) Mimouni et al. (1992) also could infer the formation of dimeric species of the type Ca_2MM from two phase extraction data, confirming the existence of such species. The differences in the equilibrium constant estimates given above and those reported in the literature perhaps reflect the importance of the medium in deciding the magnitude of these constants (Taylor et al., 1985). The species Ca_2HH , undetected in steady-state observations (Thomas et al., 1997), have not been detected from our kinetic data also. However, they could exist in membranes at small concentrations, as suggested in the undetected kinetic steps (Eqs. 17 and 18). Their stabilization could come from intermolecular hydrogen bond bridges (Deber and Pfeiffer, 1976).

Comparison with mechanisms of CAL-mediated monovalent metal ion and H^+ transport suggested in the literature

Species of the type Ca_2MH had been invoked in the literature to explain the “two-phase extraction” equilibrium data at different concentrations of H^+ and M^+ (Pfeiffer and Lardy, 1976). It had also been suggested that the CAL-mediated M^+/H^+ exchange could be similar to that by nigericin. The kinetic data discussed above support the hypothesis that Ca_2MH can be the dominant species responsible for M^+ transport when $\text{M}^+ = \text{K}^+$ and Cs^+ . However, the pH-dependent $1/\tau$ obtained with $\text{M}^+ = \text{Li}^+$ and Na^+ are not consistent with such a hypothesis and suggest the involvement of Ca_2MM for M^+ transport in these systems. Also, unlike in the nigericin-mediated M^+/H^+ exchange (Prabhananda and Ugrankar, 1991) where only monomeric species are involved, in the CAL-mediated M^+/H^+ exchange the dimeric species translocate M^+ and the monomeric Ca-H translocate H^+ (Fig. 4).

Two more kinetic studies on CAL-mediated H^+ transport in SBPL vesicle solutions containing K^+ with conclusions different from ours have appeared in the literature. Krishnamoorthy and Ahmed (1992) created ΔpH by T-jump and observed a ΔpH relaxation rate proportional to $[\text{Ca}]_0^2$ similar to that in Fig. 1. Even though they have suggested the translocation of M^+ carrying CAL-dimeric species to be rate-limiting, they have not been able to characterize the dimeric species as Ca_2KH since their studies were restricted to $\text{pH} \sim 7.5$.

In the second kinetic study, the ΔpH was created by mixing vesicle solutions at $\text{pH} \sim 7.5$ with a buffer of slightly different pH in a stopped-flow instrument (Jyoti et al., 1994). In this work, the rate-limiting step of ΔpH decay was not identified and the observed nonlinear dependence of ΔpH decay rate on $[\text{Ca}]_0$ was used to argue that the ion

transport is through channels formed by CAL aggregates in the membrane. This study suffers from severe infirmities:

1. As shown in Eq. A11, in the channel mechanism the slope of $\log(\text{transport rate})$ against $\log([\text{A23187}])$ plot should progressively decrease with increase in $[\text{A23187}]$. In the limit when almost all the CAL aggregate into channels the slope should tend toward a constant value = 1. The plot in Fig. 3 of Jyoti et al. (1994) shows quite the opposite behavior. Thus, contrary to the claim made by Jyoti et al. (1994), even their data do not support the channel mechanism.
2. In the decay traces shown in Fig. 1 *a* of Jyoti et al (1994) the “base lines” [the value of $a_0\exp(-k_{\text{app}}t)$ at infinitely long time t] are uncertain since the data have not been recorded at longer intervals of time. The drift in the amplifiers used for recording the data could also cause base line errors. The errors in the base line of exponentials could lead to large errors in the estimates of k_{app} when plots similar to Fig. 1 *b* of Jyoti et al. (1994) are used. Estimates of “initial rates” from the initial region of the decay traces also have large uncertainties. Within the limits of such errors, the data given in Fig. 2 of Jyoti et al. (1994) also show transport rates proportional to $[\text{Ca}]_0^2$ similar to those reported by Krishnamoorthy and Ahmed (1992) and in the data given above. However, the “dimeric rate-limiting species” invoked to explain such data have to be at concentrations very much smaller than $[\text{Ca}]_0$ to account for the “quadratic dependence.” Also, the dimeric species (without further aggregation) are not adequate to form channels.
3. Other independent evidence against the channel mechanism given in the literature includes the following. 1) CAL-polymeric species are at negligible concentrations in chloroform solutions (Thomas et al., 1997). 2) The model of the divalent metal ion-CAL complex does not favor channel formation (Deber and Pfeiffer, 1976). Such a model has the support from electron paramagnetic resonance data, which have helped the identification of the ligand atoms coordinating to the metal ion (Prabhananda and Kombrabail, 1994).

Rate-limiting step of CAL-mediated divalent metal ion transport

Kolber and Haynes (1981) have studied the kinetics of CAL-mediated divalent metal ion (DM^{2+}) transport across vesicular membranes by monitoring the time dependence of depletion of the divalent metal ion-bound CAL in the membrane, from fluorescence measurements. They have analyzed the data using a transport scheme with the following assumptions. 1) The Ca^{2+} -CAL complex dissociation-formation reactions and formation of Ca^{2+} -EDTA complex at the aqueous medium-membrane interface are not rate-limiting. 2) $\text{Ca}_2\text{-DM}$ translocation across the membrane is the rate-limiting step. Therefore, the validity of their estimate of $\text{Ca}_2\text{-Ca}$ translocation rate constant ($\sim 0.1\text{--}0.3\text{ s}^{-1}$) depends

on the validity of these two assumptions. The experimental observations discussed below show that both the aforementioned assumptions are not valid.

Grell and co-workers (Krause et al., 1983; Grell et al., 1984) have noted a correlation between the relative magnitudes of dissociation rate constants of the Ca^{2+} and Mg^{2+} complexes of CAL (determined from stopped-flow and T-jump relaxation studies in methanol and 30% water-methanol mixtures) and the turnover numbers for CAL-mediated Ca^{2+} and Mg^{2+} transports (Pfeiffer et al., 1978). In the "two phase extraction kinetic studies," Jeminet and co-workers (Bolte et al., 1985; Prudhomme et al., 1986) have observed large $\text{Ca}^{2+}/\text{Mg}^{2+}$ selectivity in the rate of release of DM^{2+} into the aqueous phase by the dissociation of $\text{Ca}_2\text{-DM}$ dissolved in the organic phase. Similar observations have been made even when calcimycin analogs were used. In these experiments the translocations within the organic phase could not have contributed to the $\text{Ca}^{2+}/\text{Mg}^{2+}$ selectivity, since the diffusion rates of $\text{Ca}_2\text{-DM}$ (which depend on the sizes of the complexes) are expected to be similar for both $\text{DM}^{2+} = \text{Ca}^{2+}$ and Mg^{2+} . Therefore, we conclude that the dissociation of the complex is the rate-limiting step.

From the kinetic study of $\text{Ca}_2\text{-DM}$ formation and dissociation in methanol it was possible to conclude that the rate-limiting steps of formation and dissociation mechanisms are associated with the charged complex Cal-DM^+ (Krause et al., 1983; Albrecht-Gary et al., 1989) and the coordination and dissociation of the second CAL is a fast step. The observation that the dissociation rate constant of the 1:1 complex is sensitive to the polarity of the medium (Krause et al., 1983) can be used to predict that the CAL-mediated Ca^{2+} transport rate should be lipid composition-dependent if the dissociation of this complex at the interface is the rate-limiting step. The kinetic data are consistent with this prediction (Kolber and Haynes, 1981).

Furthermore, the translocation rate constants of the electroneutral complexes $\text{Ca}_2\text{-DM}$ and Ca_2MM can be expected to be of similar magnitude ($\sim 5 \times 10^3 \text{ s}^{-1}$ determined in the present work) in view of the expected similarity in the sizes of the dimeric CAL-species. Compared to this estimate the turnover number of CAL-mediated Ca^{2+} transport ($\sim 45 \text{ s}^{-1}$) is much smaller (Pfeiffer et al., 1978). Therefore, we conclude that the translocation of $\text{Ca}_2\text{-DM}$ is not the rate-limiting step of CAL-mediated Ca^{2+} transport across the membrane, contrary to the assumption of Kolber and Haynes (1981).

In the mechanism of Fig. 4 the transfer of M^+ between Ca_2MM or Ca_2MH and the aqueous medium is a fast step. This is in contrast with the transfer of DM^{2+} to the aqueous medium by the slow dissociation of Cal-DM^+ at the interface, suggested above. Stabilization of the charged species Cal-DM^+ by coulombic interactions with the polar region of the bilayer membrane could also have contributed to such a difference in the rates at the interface.

APPENDIX

The linearized rate equations for small deviations of concentrations from equilibrium in the transport scheme of Fig. 4 can be written as follows (Prabhananda and Ugrankar, 1991).

$$-d\{\Delta[\text{H}^+]_i\}/dt = (\ln 10)\{[\text{H}^+]_i/b_i\}\{k_0(\Delta[\text{Cal-H}]_{ii} - \Delta[\text{Cal-H}]_{ei}) + f_x k_1(\Delta[\text{Ca}_2\text{MH}]_{ii} - \Delta[\text{Ca}_2\text{MH}]_{ei})\} \quad (\text{A1})$$

$$-d\{\Delta[\text{Cal}]_{ii}\}/dt = \{k_0(\Delta[\text{Cal-H}]_{ii} - \Delta[\text{Cal-H}]_{ei}) + f_x k_1(\Delta[\text{Ca}_2\text{MH}]_{ii} - \Delta[\text{Ca}_2\text{MH}]_{ei}) + k_2(\Delta[\text{Ca}_2\text{MM}]_{ii} - \Delta[\text{Ca}_2\text{MM}]_{ei})\} \quad (\text{A2})$$

where f_x is the probability for the reaction given by Eq. 16 and b_i = internal buffer capacity of vesicles. The subscripts "i," "e," "ii," and "ei" refer to concentrations inside vesicles, external to vesicles, in the inner layer of the vesicular bilayer membrane, and in the external layer of the membrane, respectively. $[\text{Cal}]_{ii}$, the total concentration of CAL in the inner layer of the membrane, is $\approx \{[\text{Cal}^-]_{ii} + [\text{Cal-H}]_{ii} + [\text{Cal-M}]_{ii}\}$, since the concentrations of the dimeric species are small compared to the monomeric species as inferred from Fig. 1. Using the parameters defined in Eqs. 4–9 we can write,

$$-d\{\Delta[\text{H}^+]_i\}/dt = (\ln 10)\{a_{11}\Delta[\text{H}^+]_i + a_{12}\Delta[\text{Cal}]_{ii}\} \quad (\text{A3})$$

$$-d\{\Delta[\text{Cal}]_{ii}\}/dt = a_{21}\Delta[\text{H}^+]_i + a_{22}\Delta[\text{Cal}]_{ii} \quad (\text{A4})$$

$$\begin{aligned} a_{11} &= \left\{ \frac{[\text{H}^+]_i}{b_i} \right\} \left\{ \left(\frac{k_0[\text{Cal}]_{ii}}{A^2} \right) \left(K_H + \frac{[\text{M}^+K_H]}{K_M} \right) \right. \\ &\quad \left. + \left(\frac{f_x k_1[\text{Ca}_2\text{MH}]_{ii}^2}{A^3} \right) \left(\frac{[\text{M}^+]}{K_{MH}} \right) \left(\frac{K_H}{K_M} \right) \left(K_H - [\text{H}^+]_i + \frac{[\text{M}^+K_H]}{K_M} \right) \right\} \\ a_{12} &= \left\{ \frac{[\text{H}^+]_i}{b_i} \right\} \left\{ \frac{2k_0[\text{H}^+]_i}{A} + \left(\frac{4f_x k_1[\text{Cal}]_{ii}}{A^2} \right) \left(\frac{[\text{M}^+][\text{H}^+]_i}{K_{MH}} \right) \left(\frac{K_H}{K_M} \right) \right\} \\ a_{21} &= \left\{ \left(\frac{k_0[\text{Cal}]_{ii}}{A^2} \right) \times \left(K_H + \frac{[\text{M}^+K_H]}{K_M} \right) + \left(\frac{f_x k_1[\text{Ca}_2\text{MH}]_{ii}^2}{A^3} \right) \right. \\ &\quad \left. \left(\frac{[\text{M}^+]}{K_{MH}} \right) \left(\frac{K_H}{K_M} \right) \times \left(K_H - [\text{H}^+]_i + \frac{[\text{M}^+K_H]}{K_M} \right) \right\} \\ &\quad - \left(\frac{2k_2}{K_{MM}} \right) \left(\frac{[\text{Cal}]_{ii}^2}{A^3} \right) \left(\frac{[\text{M}^+K_H]}{K_M} \right)^2 \\ a_{22} &= [\text{H}^+]_i \left\{ \frac{2k_0}{A} + \left(\frac{4k_1[\text{Cal}]_{ii}}{A^2} \right) \left(\frac{[\text{M}^+]}{K_{MH}} \right) \left(\frac{K_H}{K_M} \right) \right\} \\ &\quad + 4 \left(\frac{k_2}{K_{MM}} \right) \left(\frac{[\text{Cal}]_{ii}}{A^2} \right) \left(\frac{[\text{M}^+K_H]}{K_M} \right)^2 \end{aligned} \quad (\text{A5})$$

since for our experimental conditions $b_i V_i / b_e V_e \ll 1$. (b_e is the buffer capacity of the medium external to vesicles and V_i and V_e are the volumes of the aqueous medium inside and outside vesicles). The ΔpH relaxation rate, $1/\tau$, is given by Prabhananda and Ugrankar (1991),

$$1/\tau = \{\ln 10\}\{a_{11}a_{22} - a_{12}a_{21}\}/a_{22} \quad (\text{A6})$$

Substituting the expressions A5 in Eq. A6 we can write the following.

$$\begin{aligned}
 1/\tau &= (\ln 10)([H^+]_i/b_i)(F_1 + F_2 + F_3)/F_4 \\
 F_1 &= k_0 k_1 (1 - f_x)([Ca]_{ii}^2/A^2)([M^+]K_H/K_M)[H^+]_i/K_{MH} \\
 F_2 &= 2k_0 k_2 ([Ca]_{ii}^2/A^2)([M^+]K_H/K_M)^2/K_{MM} \\
 F_3 &= 2f_x k_1 k_2 ([Ca]_{ii}^3/A^3)([M^+]K_H/K_M)^3/(K_{MH}K_{MM}) \\
 F_4 &= [H^+]_i \{k_0 + 2k_1 [Ca]_{ii}/A\} ([M^+]/K_{MH})(K_H/K_M) \\
 &\quad + 2(k_2/K_{MM})[Ca]_{ii}/A ([M^+]K_H/K_M)^2 \quad (A7)
 \end{aligned}$$

Modification of Eq. A7 to include H^+ translocation by Ca_2HH

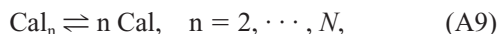
If H^+ is translocated by Ca_2HH with rate constant k_0^* in the linearized rate Eqs. A1 and A2 we should replace $k_0 \Delta[Ca-H]_{ii}$ by $\{k_0 \Delta[Ca-H]_{ii} + (k_0^*/K_{HH})\Delta[Ca-H]_{ii}^2\}$ or replace k_0 by $\{k_0 + 2[Ca-H]_{ii} k_0^*/K_{HH}\}$ in Eq. A7. Because of the similarity in the sizes of the dimeric species we can say that $k_0^* \approx k_1$ or k_2 . In our experiments H^+ translocation is a fast step and does not limit the ΔpH decay rate. For this to be satisfied, in the modified Eq. A7 we require,

$$[Ca-H]_{ii}/K_{HH} > 10 \quad \text{or} \quad [Ca_2HH]_{ii} > 10[Ca-H]_{ii}, \quad (A8)$$

if it is assumed that translocation of Ca_2HH is a dominant H^+ translocating step. Using the experimentally determined parameters that do not depend on the precise identification of the fast H^+ translocation step (Table 1), $[Ca-H]_{ii}$ can be estimated. Use of such estimates in Eq. A8 gives high $[Ca_2HH]_{ii}$ incompatible with the concentration condition required to explain the data of Fig. 1: the concentrations of dimers and other oligomers must be much smaller than those of the monomeric CAL. Therefore, the assumption used in obtaining such estimates that Ca_2HH translocates H^+ dominantly must be incorrect.

Prediction from the channel mechanism

If there are aggregation equilibria with association constants K_n ,



the concentration of CAL in the membrane before aggregation, $[Ca]_T$, can be written in terms of concentrations of various oligomers in the membrane as,

$$\begin{aligned}
 [Ca]_T &= [Ca] + 2[Ca_2] + \dots + N[Ca_N] \\
 &= [Ca] + 2K_2[Ca]^2 + \dots + NK_N[Ca]^N \quad (A10)
 \end{aligned}$$

Since $d\{\log([Ca_N])\}/d[Ca] = d\{\log([Ca_N])\}/d\{\log([Ca]_T)\} \times \{d\{\log([Ca]_T)\}/d[Ca]\}$, the slope S of the $\log([Ca_N])$ against $\log([Ca]_T)$ plot ($S = d\{\log([Ca_N])\}/d\{\log([Ca]_T)\}$) is given by

$$\begin{aligned}
 S &= \frac{K_N N [Ca]^{N-1} [Ca]_T}{([Ca_N])(1 + 4K_2[Ca] + \dots + N^2 K_N [Ca]^{N-1})} \\
 &\quad \frac{N[Ca]_T}{[Ca]_T + (2^2 - 2)[Ca_2] + \dots + (N^2 - N)[Ca_N]} \quad (A11)
 \end{aligned}$$

Equation A11 shows that S should decrease on increasing $[Ca]_T$ because of increased formation of polymeric species. If N number of molecules of CAL are needed for the formation of the ion conducting channel, in the channel mechanism the observed transport rate will be proportional to the channel concentration $[Ca_N]$. Therefore, Eq. A11 predicts that in the channel mechanism, the slope of $\log(\text{transport rate})$ against $\log([Ca]_T)$ plot should progressively decrease with increase in $[Ca]_T$.

REFERENCES

- Albrecht-Gary, A. M., S. Blanc-Parasote, D. W. Boyd, G. Dauphin, G. Jeminet, J. Juillard, M. Prudhomme, and C. Tissier. 1989. X-14885A: an ionophore closely related to calcimycin (A-23187). NMR, thermodynamic, and kinetic studies of cation selectivity. *J. Am. Chem. Soc.* 111:8598–8609.
- Balasubramanian, S. V., S. K. Sikdar, and K. R. K. Easwaran. 1992. Bilayers containing calcium ionophore A23187 form channels. *Biochem. Biophys. Res. Commun.* 189:1038–1042.
- Ben-Hayyim, G., and G. H. Krause. 1980. Transport of mono and divalent cations across chloroplast membranes mediated by the ionophore A23187. *Arch. Biochem. Biophys.* 202:546–557.
- Bolte, J., C. Demuyne, and G. Jeminet. 1985. Selectivite du transport de Ca^{++}/Mg^{++} a travers une membrane liquide par A23187 (calcimycin) et son derive N-methyle. *Can. J. Chem.* 63:3478–3481.
- Deber, C. M., and D. R. Pfeiffer. 1976. Ionophore A23187: solution conformations of the calcium complex and free acid deduced from proton and carbon-13 magnetic resonance studies. *Biochemistry.* 15: 132–140.
- Eigen, M., and L. DeMayer. 1963. Relaxation methods. In *Investigations of Rates and Reaction Mechanisms of Reactions*. S. L. Freiss, E. S. Lewis, and A. Weissberger, editors. Interscience, New York. 895–1054.
- Garlid, K. D., D. J. DiResta, A. D. Beavis, and W. H. Martin. 1986. On the mechanism by which dicyclohexylcarbodiimide and quinine inhibit K^+ transport in rat liver mitochondria. *J. Biol. Chem.* 261:1529–1535.
- Grell, E., G. Krause, E. Lewitzki, G. Mager, and H. Ruf. 1984. Specificity and dynamic aspects of cation transport systems in membranes. In *Progress in Bioorganic Chemistry and Molecular Biology*, Yu. A. Ovchinnikov, editor. Elsevier Science, Amsterdam. 239–246.
- Henderson, P. J. F., J. D. McGivan, and J. B. Chappeell. 1969. The action of certain antibiotics on mitochondrial, erythrocyte and artificial phospholipid membranes. The role of induced proton permeability. *Biochem. J.* 111:521–535.
- Jyoti, G., A. Surolia, and K. R. K. Easwaran. 1994. A23187-channel behavior: fluorescence study. *J. Biosci.* 19:277–282.
- Kauffman, R. F., R. W. Taylor, and D. R. Pfeiffer. 1982. Acid-base properties of ionophore A23187 in methanol-water solutions and bound to unilamellar vesicles of dimyristoyl-phosphatidylcholine. *Biochemistry.* 21:2426–2435.
- Kolber, M. A., and D. H. Haynes. 1981. Fluorescence study of the divalent cation transport mechanism of ionophore A23187 in phospholipid membranes. *Biophys. J.* 36:369–391.
- Krause, G., E. Grell, A. M. Albrecht-Gary, D. W. Boyd, and J. P. Schwing. 1983. Dynamic aspects of complex formation and dissociation between the antibiotic A23187 and alkaline earth cations. In *Physical Chemistry of Transmembrane Ion Motions*. G. Spach, editor. Elsevier Science, Amsterdam. 255–263.
- Krishnamoorthy, G. 1986. Temperature jump as a new technique to study the kinetics of fast transport of protons across membranes. *Biochemistry.* 25:6666–6670.
- Krishnamoorthy, G., and I. Ahmed. 1992. Rapid transport of protons across membranes: its significance measurement and control. In *Biomembrane Structure & Function—The State of the Art*. B. P. Gaber and K. R. K. Easwaran, editors. Adenine Press, New York. 195–207.
- Mimouni, M., S. Perrier, R. Frihmat, M. Hebrant, G. Jeminet, Y. Pointud, and J. Juillard. 1992. Mode of action of calcimycin (A23187). V. Its reactions with monovalent metal ions in a biphasic water-organic solvent system. *J. Chim. Phys.* 89:2169–2186.
- Nakashima, R. A., and K. D. Garlid. 1982. Quinine inhibition of Na^+ and K^+ transport provides evidence for two cation/ H^+ exchangers in rat liver mitochondria. *J. Biol. Chem.* 257:9252–9254.

- Ortiz-Carranza, O., M. E. Miller, N. C. Adranga, and P. K. Lauf. 1997. Alkaline pH and internal calcium increase Na^+ and K^+ effluxes in LK sheep red blood cells in Cl^- free solutions. *J. Membr. Biol.* 156: 287–295.
- Pfeiffer, D. R., and H. A. Lardy. 1976. Ionophore A23187: the effect of H^+ concentration on complex formation with divalent and monovalent cations and demonstration of K^+ transport in mitochondria mediated by A23187. *Biochemistry*. 15:935–943.
- Pfeiffer, D. R., P. W. Reed, and H. A. Lardy. 1974. Ultraviolet and fluorescent spectral properties of the divalent cation ionophore A23187 and its metal ion complexes. *Biochemistry*. 13:4007–4014.
- Pfeiffer, D. R., R. W. Taylor, and H. A. Lardy. 1978. Ionophore A23187: cation binding and transport properties. *Ann. NY. Acad. Sci.* 307: 402–423.
- Prabhananda, B. S., and M. H. Kombrabail. 1992. Monensin-mediated transport of H^+ , Na^+ , K^+ and Li^+ ions across vesicular membranes: T-jump studies. *Biochim. Biophys. Acta.* 1106:171–177.
- Prabhananda, B. S., and M. H. Kombrabail. 1994. Identification of coordinating ligand atoms in $\text{Cu}(\text{calcimycin})_2$ from EPR linewidths in chloroform solutions. *J. Magn. Reson. B.* 105:167–171.
- Prabhananda, B. S., and M. H. Kombrabail. 1995. Enhancement of rates of H^+ , Na^+ and K^+ transport across phospholipid vesicular membrane by the combined action of carbonyl cyanide m-chlorophenylhydrazone and valinomycin: temperature jump studies. *Biochim. Biophys. Acta.* 1235: 323–335.
- Prabhananda, B. S., and M. H. Kombrabail. 1996. Two mechanisms of H^+/OH^- transport across phospholipid vesicular membrane facilitated by gramicidin A. *Biophys. J.* 71:3091–3097.
- Prabhananda, B. S., and M. M. Ugrankar. 1991. Nigericin-mediated H^+ , K^+ and Na^+ transports across vesicular membrane: T-jump studies. *Biochim. Biophys. Acta.* 1070:481–491.
- Prudhomme, M., G. Dauphin, and G. Jeminet. 1986. Semi-synthesis of A23187 (calcimycin) analogs. III. Modification of benzoxazole ring substituents, ionophorous properties in an organic phase. *J. Antibiotics.* 39:922–933.
- Reed, P. W., and H. A. Lardy. 1972. A23187 a divalent cation ionophore. *J. Biol. Chem.* 247:6970–6977.
- Taylor, R. W., C. J. Chapman, and D. R. Pfeiffer. 1985. Effect of membrane association on the stability of complexes between ionophore A23187 and monovalent cations. *Biochemistry*. 24:4852–4859.
- Thomas, T. P., E. Wang, D. R. Pfeiffer, and R. W. Taylor. 1997. Evidence against formation of A23187 dimers and oligomers in solution: photo-induced degradation of ionophore A23187. *Arch. Biochem. Biophys.* 342:351–361.